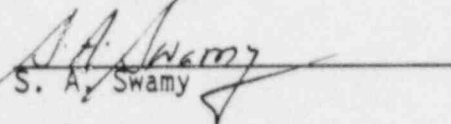


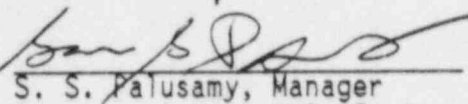
MT-SME-200

EVALUATION OF AN INDICATION IN THE
BRAIDWOOD UNIT 2 LOOP 1
ELBOW TO VALVE WELD REGION

APRIL 1988

Y. S. Lee
W. H. Bamford
F. J. Witt
E. R. Johnson

Verified by: 
S. A. Swamy

Approved by: 
S. S. Palusamy, Manager
Structural Materials Engineering

Although information contained in this report is non-proprietary, no distribution shall be made outside Westinghouse or its licensees without the customer's approval.

WESTINGHOUSE ELECTRIC CORPORATION
Generation Technology Systems Division
P.O. Box 2728
Pittsburgh, Pennsylvania 15230-2728

TABLE OF CONTENTS

Section	Title	Page
1.0	INTRODUCTION AND CRITERIA	1-1
	1.1 Introduction	1-1
	1.2 Code Acceptance Criteria - Stainless Steel	1-1
2.0	LOADING CONDITIONS AND STRESS ANALYSIS	2-1
	2.1 Transients	2-1
	2.2 Pipe loadings	2-2
3.0	FRACTURE ANALYSIS METHODS AND MATERIAL PROPERTIES	3-1
	3.1 Fracture Toughness	3-1
	3.2 Allowable Flaw Size Determination	3-1
	3.3 Stress Corrosion Cracking Susceptibility	3-2
	3.4 Thermal Aging	3-3
4.0	FATIGUE CRACK GROWTH	4-1
	4.1 Analysis Methodology	4-1
	4.2 Stress Intensity Factor Calculations	4-1
	4.3 Crack Growth Rate Reference Curves	4-3
5.0	FLAW EVALUATION RESULTS	5-1
	5.1 IWB 3640 Evaluation	5-1
	5.2 Fracture Mechanics Evaluation	5-2
6.0	DISCUSSION AND CONCLUSIONS	6-1
7.0	REFERENCES	7-1
APPENDIX A	FLAW EVALUATION CHARTS	A-1

SECTION 1.0
INTRODUCTION AND CRITERIA

1.1 INTRODUCTION

During preservice ultrasonic inspection on Braidwood Unit 2 in 1987, an indication was detected in the elbow to valve weld region (weld number 2RC-01-04). A near surface indication was detected on the elbow side of the static cast austenitic stainless steel elbow to loop isolation valve weld. The ultrasonic examination was performed using a dual element nominal 45° refracted L-wave transducer. The indication size was determined to be 1.5 inches long and 0.51 inches deep, oriented circumferentially and very close to the weld root, but not breaking through to the inside surface. Subsequent penetrant examinations performed on the inside surface revealed no indications, confirming the indication to be subsurface.

Review of the construction radiographs identified a shrinkage type flaw acceptable to the ASME Code Section III Construction Code radiographic standards in this region. Ultrasonic examination performed to detect the axial component of the flaw was restricted due to the weld crown geometry. Therefore it is assumed that the indication extends no greater than 0.8 inches in length axially and 0.51 inches deep.

To ensure the indications do not compromise the integrity of the reactor coolant system even in the unlikely event that they were actually flaws, a fracture evaluation has been carried out, using the rules of ASME Code Section XI, paragraph IWB 3600 for both the circumferential and axial orientations. The indications are in the steam generator stainless steel inlet elbow near the weld. Both weld metal and base metal locations are considered in this analysis.

1.2 CODE ACCEPTANCE CRITERIA - STAINLESS STEEL

The evaluation procedures and acceptance criteria for indications in austenitic stainless piping are contained in paragraph IWB 3640 of ASME Section XI.^[1] The evaluation is applicable to all the materials within a specified

distance from the weld centerline, \sqrt{rt} , where r = the pipe nominal outside radius and t is the wall thickness. For the inlet elbow to valve region, this distance is calculated to be 6.2 inches, which encompasses regions of the elbow and weld including the flaw indications given in figure 1.1.

The evaluation process begins with a flaw growth analysis, with the requirement to consider growth due to both fatigue and stress corrosion cracking. For pressurized water reactors only fatigue crack growth need be considered, as discussed in section 4.3. The methodology for the fatigue crack growth analysis is described in detail in section 4.

The calculated maximum flaw dimensions at the end of the evaluation period are then compared with the maximum allowable flaw dimensions for both normal operating conditions and emergency and faulted conditions, to determine acceptability for continued service. Provisions are made for considering flaws projected both circumferentially and axially.

In IWB 3640 the allowable flaw sizes have been defined in the tables based on maintaining specified safety margins on the loads at failure. These margins are 2.77 for normal and upset conditions and 1.39 for emergency and faulted conditions. The calculated failure loads are different for the base metal and the flux welds, which have different fracture toughness values, as discussed in section 4.3. The failure loads, and consequently the allowable flaw sizes, are larger for the base metal than for the welds. Allowable flaw sizes for welds are contained in separate tables, in IWB 3640.

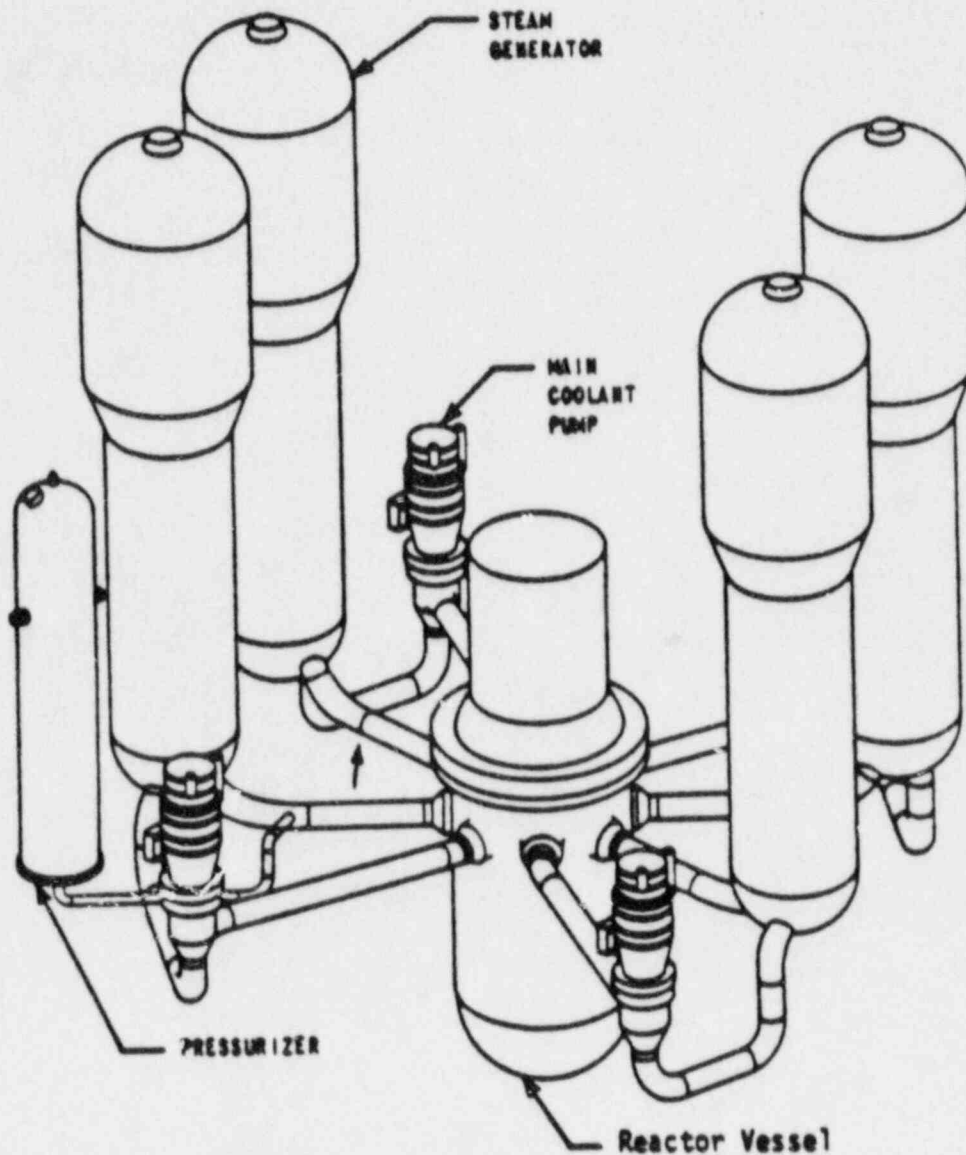


Figure 1-1. Geometry and Location of Inlet Nozzle Elbow to Pipe Weld
 (Arrow shows approximate location of indication, adjacent
 to the isolation valve weld which is not shown)

SECTION 2.0 LOADING CONDITIONS AND STRESS ANALYSIS

In performing the analyses necessary to determine allowable flaw depths and fatigue crack growth for the flaw evaluation process, it is important that all the applicable loadings be considered. Clearly the applicable design transients must be considered, but other loadings are also important. The residual stresses which exist in the region of interest have been considered. Note that for thinner sections these stresses are negligible, but for thick walled vessels, and regions not stress-relieved, the stresses are important. There is another loading which must be considered, and that is the piping loads, which must be used in piping systems and connections to piping.

2.1 TRANSIENTS

The key parameters used in the evaluation of indications discovered during inservice inspection are two critical flaw depths. The first of these critical flaw depths is calculated using stresses from governing normal, upset, and test conditions. The second is calculated based on stresses for the governing emergency and faulted conditions. Allowable flaw depths are calculated based on these two sets of conditions from the ASME Code criteria.

The design transients and the number of occurrences for the design life of the components are required for the stress, fracture and fatigue crack growth analyses. The design transients for the Braidwood Unit 2 primary system are contained in table 2-1. Both the critical flaw size and the fatigue crack growth used in flaw evaluation are functions of the stresses at the cross-section where the flaw of interest is located, and the material properties. Therefore, the first step for the evaluation of a flaw is to determine the appropriate limiting load conditions for the location of interest. This has been done, and is discussed in section 2.2.

2.2 PIPE LOADINGS

The loading conditions which were evaluated include thermal expansion (normal and upset), pressure, deadweight and seismic (OBE and SSE) loadings. The forces and moments for each condition were obtained from the ASME Code Section III calculations previously performed by Westinghouse. Residual stresses were not used in this portion of the evaluation, in compliance with the Code guidelines. Stresses as appropriate were used in the fatigue crack growth analysis, as discussed in Section 4.0. The stress intensity values were calculated using the following equations:

$$SI = P_m + P_b$$

$$SI = \frac{F_x}{A} + \frac{1}{Z} [M_x^2 + M_y^2 + M_z^2]^{0.5}$$

where

- F_x = axial force component (membrane)
- M_x, M_y, M_z = moment components (bending)
- A = cross-section area
- Z = section modulus

The section properties A and Z at the weld location were determined based on the minimum pipe dimensions: inside diameter of 29.0 inches, wall thickness of 2.45 inches. This is conservative since the measured wall thickness at the weld is 2.55 inches.

The following load combinations were used.

A. Normal/Upset - Primary Stress

Pressure + Deadweight + OBE

B. Emergency/Faulted - Primary Stress

Pressure + Deadweight + SSE

C. Expansion Stress - Secondary Stress

- i) Normal Thermal
- ii) Upset Thermal

D. Normal/Upset - Total Stress

- i) Pressure + Deadweight + OBE + Normal Thermal
- ii) Pressure + Deadweight + Upset Thermal

E. Emergency/Faulted - Total Stress

- i) Pressure + Deadweight + SSE + Normal Thermal
- ii) Pressure + Deadweight + Faulted Thermal

In D and E above, load combination (i) is the governing case. The results below are based on the normal thermal loading conditions.

Results

The governing maximum stress intensity values are summarized below:

<u>Condition</u>	<u>P_m</u> Primary Membrane Stress (ksi)	<u>$P_m + P_b$</u> Primary Membrane + Bending Stress (ksi)	<u>P_e</u> Expansion Stress (ksi)
Normal/Upset			
Circumferential indications	7.77	10.23	4.48
Axial indications	15.54	15.54	0.0
Emergency/Faulted			
Circumferential indications	9.20	14.93	4.48
Axial indications	18.4	18.4	0.0

TABLE 2-1
SUMMARY OF PRIMARY SYSTEM TRANSIENTS - BRAIDWOOD UNIT 2

<u>TRANSIENT NUMBER</u>	<u>TRANSIENT IDENTIFICATION</u>	<u>SPECIFIED CYCLES</u>
1	Partial loss of flow	80
2	Inadvertant S.I. Actuation	60
3	Heatup	200
4	Cooldown	200
5	Unit loading at 5% per minute	13200
6	Unit unloading at 5% per minute	13200
7	10% step load increase	2000
8	10% step load decrease	2000
9	Large step load decrease with steam dump	200
10	Feedwater cycling at hot shutdown	2000
11	Loop out-of-service, normal loop startup	70
12	Loop out-of-service, normal loop shutdown	80
13	Reactor trip from full power -- no cooldown	230
14	Reactor trip from full power -- cooldown, no S.I.	160
15	Reactor trip from full power -- cooldown and S.I.	10
16	Inadvertant startup of an inactive loop -- inactive loop	10
17	Inadvertant startup of an inactive loop -- active loop	10
18	Small LOCA (E/F)	5
19	Small steam line break (E/F)	5
20	Complete loss of flow (E/F)	5
21	Turbine roll test -- heat up	20

TABLE 2-1 (Cont'd.)
 SUMMARY OF PRIMARY SYSTEM TRANSIENTS - BRAIDWOOD UNIT 2

<u>TRANSIENT NUMBER</u>	<u>TRANSIENT IDENTIFICATION</u>	<u>SPECIFIED CYCLES</u>
22	Turbine roll test -- cooldown	20
23	Loss of load	80
24	Control rod drop	80
25	Loss of power	40
26	Inadvertant RCS depressurization	20
27	Unit loading at 5% per minute for 0 to 15% power	13200
28	Unit unloading at 5% per minute for 0 to 15% power	13200
29	Steady state fluctuation	150000

SECTION 3.0
FRACTURE ANALYSIS METHODS AND MATERIAL PROPERTIES

3.1 FRACTURE TOUGHNESS

The inlet elbow is cast stainless steel SA351, type CF8A. The pipe to elbow weld was made by a shielded metal arc process.

The fracture toughness of the base metal has been found to be very high, even at operating temperatures [2], where the J_{IC} values have been found to be well over 2000 in lb/in². Fracture toughness values for weld materials have been found to display much more scatter, with the lowest reported values significantly lower than the base metal toughness. Although the J_{IC} values reported have been lower, the slope of the J-R-curve is still large for these lower J_{IC} cases. Representative values for J_{IC} were obtained from the results of Landes and co-workers [3], where the following value was obtained, and was used in the development of the fracture evaluation methods.

for shield metal arc welds: $J_{IC} = 990$ in lb/in².

3.2 ALLOWABLE FLAW SIZE DETERMINATION

The critical flaw size is not directly calculated as part of the flaw evaluation process for stainless steels. Instead, the failure mode and critical flaw size are incorporated directly into the flaw evaluation technical basis, and therefore into the tables of "Allowable End-of-Evaluation Period Flaw Depth to Thickness Ratio," which are contained in paragraph IWB 3640.

Rapid, nonductile failure is possible for ferritic materials at low temperatures, but is not applicable to stainless steels. In stainless steel materials, the higher ductility leads to two possible modes of failure, plastic collapse or unstable ductile tearing. The second mechanism can occur

when the applied J integral exceeds the J_{Ic} fracture toughness, and some stable tearing occurs prior to failure. If this mode of failure is dominant, the load carrying capacity is less than that predicted by the plastic collapse mechanism.

The allowable flaw sizes of paragraph IWB 3640 for the high toughness base materials were determined based on the assumption that plastic collapse would be achieved and would be the dominant mode of failure. However, due to the reduced toughness of the submerged arc and shielded metal arc welds, it is possible that crack extension and unstable ductile tearing could occur and be the dominant mode of failure. This consideration in effect reduces the allowable end of interval flaw sizes for flux welds relative to the austenitic wrought piping, and has been incorporated directly into the evaluation tables.

3.3 STRESS CORROSION CRACKING SUSCEPTIBILITY

In evaluating flaws, all mechanisms of subcritical crack growth must be evaluated to ensure that proper safety margins are maintained during service. Stress corrosion cracking has been observed to occur in stainless steel in operating BWR piping systems; the discussion presented here is the technical basis for not considering this mechanism in the present analysis.

For all Westinghouse plants, there is no history of cracking failure in the reactor coolant system loop piping. For stress corrosion cracking (SCC) to occur in piping, the following three conditions must exist simultaneously: high tensile stresses, a susceptible material, and a corrosive environment. Since some residual stresses and some degree of material susceptibility exist in any stainless steel piping, the potential for stress corrosion is minimized by proper material selection immune to SCC as well as preventing the occurrence of a corrosive environment. The material specifications consider compatibility with the system's operating environment (both internal and external) as well as other materials in the system, applicable ASME Code rules, fracture toughness, welding, fabrication, and processing.

The environments known to increase the susceptibility of austenitic stainless steel to stress corrosion are oxygen, fluorides, chlorides, hydroxides, hydrogen peroxide, and reduced forms of sulfur (e.g., sulfides, sulfites, and thionates). Strict pipe cleaning standards prior to operation and careful control of water chemistry during plant operation are used to prevent the occurrence of a corrosive environment. Prior to being put into service, the piping is cleaned internally and externally. During flushes and preoperational testing, water chemistry is controlled in accordance with written specifications. External cleaning for Class 1 stainless steel piping includes patch tests to monitor and control chloride and fluoride levels. For preoperational flushes, influent water chemistry is controlled. Requirements on chlorides, fluorides, conductivity, and pH are included in the acceptance criteria for the piping.

During plant operation, the reactor coolant system (RCS) water chemistry is monitored and maintained within very specific limits. Contaminant concentrations are kept below the thresholds known to be conducive to stress corrosion cracking with the major water chemistry control standards being included in the plant operating procedures as a condition for plant operation. For example, during normal power operation, oxygen concentration in the RCS is expected to be less than 0.005 ppm by controlling charging flow chemistry and maintaining hydrogen in the reactor coolant at specified concentrations. Halogen concentrations are also stringently controlled by maintaining concentrations of chlorides and fluorides within the specified limits. This is assured by controlling charging flow chemistry and specifying proper wetted surface materials.

3.4 THERMAL AGING

Thermal aging at operating temperatures of reactor primary piping can reduce the fracture toughness of cast stainless steels and, to a lesser degree, stainless steel weldments. The cast stainless steel piping and elbows of the primary loop are very tough, usually exhibiting J_{Ic} values exceeding 2000 in-lb/in² and a tearing modulus, T_{mat} , well over 200. NRC procedures exist for addressing the impact of thermal aging on fracture toughness for

full-service life. The approved procedures were applied to the steam generator inlet elbow containing the indication. The elbow was fabricated of CF8A cast stainless steel, which is in general less susceptible to thermal aging than other types which contain molybdenum. It was found that the elbow qualified for the highest assignable end-of-service fracture toughness values by the NRC-approved procedure, specifically, $J_{Ic} = 750 \text{ in-lb/in}^2$, $T_{mat} = 60$.

Even with thermal aging, equivalent to full service for SMAW welds, the tearing modulus remains high (>100) and the unaged toughness, J_{Ic} , is not significantly reduced. Therefore the value of $J_{Ic} = 990 \text{ in-lb/in}^2$ from ASME Code Section XI was retained for this analysis. Because of the larger tearing modulus, SMAW welds with full service life aging remain as good as the elbow material in question from a stability view point.

Thus, the fracture toughness values applicable for full service life are $J_{Ic} = 750 \text{ in-lb/in}^2$, $T_{mat} = 60$ for the elbow, and $J_{Ic} = 990 \text{ in-lb/in}^2$ and $T_{mat} = 100$ for the SMAW weld. It should be recognized that these values are believed to be very conservative estimates of the end of life fracture properties.

SECTION 4.0 FATIGUE CRACK GROWTH

In applying the ASME Code Section XI acceptance criteria, the final flaw size a_f used in the criteria is defined as the flaw size to which the detected flaw is calculated to grow at the end of the design life, or until the next inspection time.

To determine the fatigue crack growth in the elbow to valve weld region, an analysis was carried out for the actual location of interest. The loadings used included thermal and deadweight piping loads, pressure and thermal transient loads, and residual stresses. Thermal aging has been shown not to impact fatigue crack growth, so the reference crack growth curve was not changed, as discussed further in Section 4.3.

4.1 ANALYSIS METHODOLOGY

The analysis procedure involves postulating an initial flaw at each specific region and predicting the growth of that flaw due to an imposed series of loading transients. The input required for a fatigue crack growth analysis is basically the information necessary to calculate the parameter ΔK_I (range of stress intensity factor) which depends on crack and structure geometry and the range of applied stresses in the area where the crack exists. Once ΔK_I is calculated, the growth due to that particular stress cycle can be calculated by equations given in section 4.4. This increment of growth is then added to the original crack size, and the analysis proceeds to the next transient. The procedure is continued in this manner until all the transients known to occur in the period of evaluation have been analyzed.

The transients considered in the analysis are all the design transients contained in the equipment specification, as shown for example in section 2, table 2-1. These transients are spread equally over the design lifetime of

the plant, with the exception that the preoperational tests are considered first. Faulted conditions are not considered because their frequency of occurrence is too low to affect fatigue crack growth.

4.2 RESIDUAL STRESSES

Since the piping weld of interest here was not stress-relieved, residual stresses are clearly present. For fatigue crack growth analyses, these stresses were included directly, using as a guide the residual stress values in the technical basis document for the ASME Code flaw evaluation procedures [4].

Although there is significant residual stress variation from one weldment to another, there have been a large number of measurements made, and these were collected in reference [4]. The resulting guidelines are summarized in figure 4-1. These stresses were used directly in the analysis, except in a few instances where the elastically calculated stresses were significantly above yield stress. In these cases it would be unrealistic to add the residual stresses, so they were not used. It should be noted here that the residual stresses were added to both the maximum and minimum stresses, and therefore do not affect the stress range. Their effect is seen only through the R ratio, as illustrated in section 4.4.

4.3 STRESS INTENSITY FACTOR EXPRESSIONS

Stress intensity factors were calculated from methods available in the literature for each of the flaw types analyzed. The surface flaw with aspect ratio 6:1 is analyzed using an expression developed by McGowan and Raymond [5] where the stress intensity factor K_I is calculated from the actual stress profile through the wall at the location of interest.

The maximum and minimum stress profiles corresponding to each transient are represented by a third order polynomial such that:

$$\sigma(x) = A_0 + A_1 \frac{x}{t} + A_2 \frac{x^2}{t^2} + A_3 \frac{x^3}{t^3}$$

The stress intensity factor $K_I(\phi)$ can be calculated anywhere along the crack front. The point of maximum crack depth is represented by $\phi = 0$. The following expression is used for calculating $K_I(\phi)$.

$$K_I(\phi) = \left(\frac{\pi a}{Q}\right)^{0.5} (\cos^2 \phi + \frac{a^2}{c^2} \sin^2 \phi)^{1/4} (A_0 H_0 + \frac{2a}{\pi t} A_1 H_1 + \frac{1}{2} \frac{a^2}{t^2} A_2 H_2 + \frac{4}{3\pi} \frac{a^3}{t^3} A_3 H_3)$$

The magnification factors H_0 , H_1 , H_2 and H_3 are a function of ϕ and are obtained by the procedure outlined in reference [5].

The stress intensity factor for a continuous surface flaw was calculated using an expression for an edge cracked plate [6]. The stress distribution is linearized through the wall thickness to determine the membrane and bending stresses; the applied K_I is calculated from:

$$K_I = \sigma_m Y_m (\pi a)^{0.5} + \sigma_B Y_B (a\pi)^{0.5}$$

The magnification factors Y_m and Y_B are taken from [6] and "a" is the crack depth.

4.4 CRACK GROWTH RATE REFERENCE CURVES

There is presently no reference fatigue crack growth rate curve in the ASME Code for austenitic stainless steels. However, a great deal of work has been done recently which supports the development of such a curve. An extensive study was done by the Metals Property Council working group on reference fatigue crack growth concerning the crack growth behavior of these steels in air environments, published in reference [7]. A reference curve for stainless steels in air environments, based on this work, will appear in the 1988 Addenda of Section XI.

A compilation of data for austenitic stainless steels in a PWR water environment was made by Bamford [8], and it was found that the effect of the environment on the crack growth rate was very small. From this information it was estimated that the environmental factor should be conservatively set at 2.0 in the crack growth rate equation from reference [7]. Therefore the crack growth rate equation used in the analysis was:

$$\frac{da}{dn} = C F S E \Delta K^{3.30}$$

where: C = 2.42×10^{-20}
 F = frequency factor (F = 1.0 for temperatures below 800°F)
 S = R ratio correction (S = 1.0 for R = 0; S = 1 + 1.8R for 0 < R < .8; and S = -43.35 + 57.97R for R > 0.8)
 E = environmental factor (E = 2.0 for PWR environment)
 ΔK = range of stress intensity factor, in psi $\sqrt{\text{in}}$

and R is the ratio of the minimum K_I to the maximum K_I .

4.5 FATIGUE CRACK GROWTH RESULTS

The results of the crack growth analysis work are shown in Tables 4-1 through 4-3. Table 4-1 shows results for circumferential surface flaws of two different aspect ratios, while Table 4-2 shows the results for longitudinal flaws. The top entry of each table is for an indication extending entirely around or along the pipe, while the table below is for an indication with length six times its depth. It is clear from these tables that as the indication becomes shorter relative to its depth, the crack growth will be smaller than that shown in the bottom table. For example, a flaw 0.5 inch deep and oriented longitudinally with aspect ratio of 1 to 3, say, would grow to a depth of less than 0.567 inches in ten years.

The actual indication is embedded, and thus the crack growth would be even less than the bounding number shown in Tables 4-1 or 4-2. Table 4-3 shows that crack growth for a buried flaw near the inside surface would actually be negligible.

TABLE 4-1
 FATIGUE CRACK GROWTH FOR SURFACE FLAWS - STAINLESS STEEL
 CIRCUMFERENTIAL FLAWS

	Initial Crack Depth (inches)	Crack Depth After Year			
		10	20	30	40
Continuous Flaw	0.200	0.22190	0.23964	0.25935	0.28200
	0.300	0.34070	0.37768	0.42149	0.47626
	0.400	0.46431	0.52982	0.61431	0.74043
	0.500	0.59504	0.70957	0.89247	1.30579
Aspect Ratio 1:6	0.100	0.10419	0.10719	0.11029	0.11357
	0.150	0.15743	0.16290	0.16857	0.17462
	0.200	0.21091	0.21915	0.22773	0.23694
	0.300	0.31889	0.33423	0.35048	0.36823
	0.600	0.64817	0.69568	0.74867	0.81055
	0.900	0.99008	1.09058	1.20735	1.35240

TABLE 4-2
 FATIGUE CRACK GROWTH FOR SURFACE FLAWS - STAINLESS STEEL
 LONGITUDINAL FLAWS

	Initial Crack Depth (inches)	Crack Depth After Year			
		10	20	30	40
Continuous Flaw	0.100	0.10465	0.10925	0.11415	0.11951
	0.150	0.15918	0.16866	0.17913	0.19111
	0.200	0.21602	0.23407	0.25579	0.28336
	0.300	0.34396	0.41154	0.54528	1.06241
	0.400	0.52242	0.92828	-- ^a	--
Aspect Ratio 1:6	0.1	0.10236	0.10461	0.10692	0.10934
	0.2	0.20732	0.21479	0.22276	0.23145
	0.3	0.31743	0.33716	0.36029	0.38820
	0.4	0.43755	0.48471	0.54588	0.62728
	0.5	0.56659	0.65486	0.77101	0.91586
	1.0	1.1755	1.39545	1.82326	--

^aGrowth through the wall.

TABLE 4-3
 FATIGUE CRACK GROWTH FOR CIRCUMFERENTIAL
 EMBEDDED FLAWS - STAINLESS STEEL

	Semi-initial Crack Depth (inches)	Crack Depth After Year			
		10	20	30	40
$\delta = 0.1613$	0.050	0.05105	0.05182	0.05261	0.05343
	0.070	0.07190	0.07331	0.07475	0.07626
	0.080	0.08242	0.08421	0.08605	0.08799
	0.100	0.10364	0.10634	0.10914	0.11212
$\delta = 0.242$	0.050	0.05087	0.05156	0.05226	0.05299
	0.100	0.10293	0.10524	0.10762	0.11013
	0.150	0.15602	0.16071	0.16560	0.17087
	0.180	0.16683	0.17214	0.17771	0.18372
$\delta = 0.3225$	0.050	0.05073	0.05136	0.05199	0.05264
	0.100	0.10244	0.10450	0.10661	0.10884
	0.150	0.15508	0.15933	0.16374	0.16845
	0.200	0.20874	0.21600	0.22363	0.23192
$\delta = 0.4838$	0.100	0.10196	0.10382	0.10571	0.10770
	0.150	0.15395	0.15769	0.16152	0.16561
	0.200	0.20657	0.21273	0.21910	0.22595
	0.250	0.25963	0.26853	0.27784	0.28796
	0.300	0.31372	0.32625	0.33953	0.35415
$\delta = 0.645$	0.100	0.10162	0.10327	0.10492	0.10668
	0.150	0.15328	0.15660	0.15998	0.16360
	0.200	0.20545	0.21096	0.21663	0.22274
	0.250	0.25813	0.26634	0.27486	0.28411
	0.300	0.31134	0.32274	0.33467	0.34773

Note: $\delta = S + a$, distance from the inside surface to the center line of the flaw.

Wall Thickness	Through-Wall Residual Stress ¹	
	Axial	Circumferential ²
<1 inch		
≥1 inch	See Note 3	

¹ S = 30 ksi

² Considerable variation with weld heat input.

³ $\sigma = \sigma_i [1.0 - 6.91 (a/t) + 8.69 (a/t)^2 - 0.48 (a/t)^3 - 2.03 (a/t)^4]$

σ_i = stress at inner surface (a = 0)

Figure 4-1. Recommended Axial and Circumferential Residual Stress Distributions for Austenitic Stainless Steel Pipe Welds (from reference 4)

Emergency and Faulted;	<u>Circumferential</u> <u>Indications</u>	<u>Axial</u> <u>Indications</u>
	$P_m = 9.20$ ksi	18.4 ksi
	$P_b = 5.73$	0.0
	$P_e = 4.48$	0.0

Results:

- 1) For the elbow, the allowable circumferential flaw depth from Section XI paragraph IWB 3640 is 1.9 inches for both normal/upset and emergency/faulted loads. This compares with the final flaw depth of the known flaw after crack growth of 0.53 inches after ten years.
- 2) For the elbow, the allowable axial flaw depth from IWB 3640 is 1.9 in. for both normal/upset and emergency/faulted loads. This compares with the final axial flaw depth of 0.567 inches after ten years.
- 3) For the SMAW weld, the allowable circumferential flaw depth from IWB 3640 is 1.55 in. for both normal/upset and emergency/faulted loads.

5.2 FRACTURE MECHANICS DISCUSSION

As previously discussed, the fracture toughness used for the base metal is the highest allowed for full service life thermal aging considerations. With little service temperature experience for the piping system, embrittlement by thermal aging has, at worst, only initiated; thus for the present and up at least to 1 EFPY (judgementally, based on experimental results), unaged toughness results should prevail. For the small flaw size and faulted load condition the actual applied value of J is estimated to be less than 500 in-lb/in².

SECTION 6.0
DISCUSSION AND CONCLUSIONS

A fracture evaluation has been carried out for the steam generator inlet elbow to valve weld for Braidwood Unit 2, to assess the acceptability of an indication found there. The indication is believed to be a casting defect in the elbow. To provide a complete treatment of the indication as it was characterized by a number of inspections, two different analyses were done. The first analysis considered the largest circumferential projection of the indication from all the inspections, while the second analysis considered the largest axial projection of the indication. The indication was considered to be in the elbow material but was also evaluated as if it were in the weld material.

The dimensions of the indication used in the evaluation were as follows:

Circumferential Projection: 0.5" deep x 1.5" long
Axial Projection: 0.5" deep x 0.8" long

This indication was subjected to a fatigue crack growth analysis to determine its projected growth during service. As shown in table 4-1, a circumferential crack with a depth of 0.5 inch would grow at most to a depth of 0.60 inch in ten years. This projected crack growth is expected to be very conservative, since it was calculated for a continuous surface flaw which is more elongated as compared to actual 3:1 circumferential aspect ratio. An axial flaw with a depth of 0.5 and 6:1 aspect ratio inches was calculated to grow to a depth of 0.57 inches after ten years, which is also conservative.

The actual indication is an embedded flaw and not exposed to the water environment. A consideration of embedded flaws shows that the projected crack growth is very small, over even for a forty year period.

Allowable flaw sizes for both circumferential and axial orientations were determined, and both the cast elbow and the shielded metal arc weld (SMAW) were considered. The most governing of the circumferential flaw calculations was for the weld, which had an allowable surface flaw depth of 1.55 inches as compared to an embedded indication having a depth of 0.5 inch. Therefore we see that the circumferential projection of the indication is acceptable by a wide margin.

Consideration was also given to the axial orientation, and the allowable depth was 1.9 inches. It is therefore evident that the indication in the elbow-to-valve weld is acceptable to the requirements of Section XI by a wide margin.

SECTION 7.0
REFERENCES

1. ASME Code Section XI, "Rules of Inservice Inspection of Nuclear Power Plant Components," 1983 edition (used for updated code allowable limits); 1986 edition (used for stainless steel flaw evaluation).
2. Bamford, W. H. and Bush, A. J., "Fracture of Stainless Steel," in Elastic Plastic Fracture, ASTM STP 668, 1979.
3. Landes, J. D., and Norris, D. M., "Fracture Toughness of Stainless Steel Piping Weldments," presented at ASME Pressure Vessel Conference, 1984.
4. "Evaluation of Flaws in Austenitic Steel Piping," Trans ASME, Journal of Pressure Vessel Technology, Vol. 108, Aug. 1986, pp. 352-366.
5. McGowan, J. J. and Raymund, M., "Stress Intensity Factor Solutions for Internal Longitudinal Semi-elliptic Surface Flaw in a Cylinder Under Arbitrary Loading," ASTM STP 677, 1979, pp. 365-380.
6. Plane Strain Crack Toughness Testing of High Strength Metallic Materials, ASTM STP 410, March 1969.
7. James, L. A., and Jones, D. P., "Fatigue Crack growth Correlations for Austenitic Stainless Steel in Air," in Predictive Capabilities in Environmentally Assisted Cracking," ASME publication PVP-99, Dec. 1985.
8. Bamford, W. H., "Fatigue Crack Growth of Stainless Steel Piping in a Pressurized Water Reactor Environment," Trans ASME, Journal of Pressure Vessel technology, Feb. 1979.

APPENDIX A
FLAW EVALUATION CHARTS

A-1 INTRODUCTION

The ultrasonic inspection of the Braidwood Unit 2 elbow to valve weld revealed an indication in the region of the weld-elbow interface. A fracture mechanics analysis has been documented in the main body of this report, which shows that the indication is acceptable without repair even if it were to be a crack.

In order to make the fracture evaluations performed here useful for future inspections of this region, this Appendix contains flaw evaluation charts for both surface and embedded flaws. These charts allow a determination of the acceptability of any future indications, using only the inspection results.

A-2 EVALUATION OF INDICATIONS USING THE FLAW CHARTS

A-2.1 Evaluation Procedure

The evaluation procedures contained in ASME Section XI are clearly specified in paragraph IWB-3600. Use of the evaluation charts herein follows these procedures directly, but the steps are greatly simplified.

Once the indication is discovered, it must be characterized as to its location, length (l) and depth dimension (a for surface flaws, $2a$ for embedded flaws), including its distance from the inside surface (S) for embedded indications. This characterization is discussed in further detail in paragraph IWA 3000 of Section XI.

The following parameters must be calculated from the above dimensions to use the charts (see figure A-1):

- o Flaw Shape parameter, $\frac{a}{l}$
- o Flaw depth parameter, $\frac{a}{t}$
- o Surface proximity parameter (for embedded flaws only), $\frac{\delta}{t}$

where

- t = wall thickness of region where indication is located
- l = length of indication
- a = depth of surface flaw; or half depth of embedded flaw in the width direction
- δ = distance from flaw centerline to surface (for embedded flaws only) ($\delta = S + a$)
- S = smallest distance from edge of embedded flaw to surface

Once the above parameters have been calculated and the determination made as to whether the indication is embedded or on the surface, then the two parameters may be plotted directly on the appropriate evaluation chart. Its location on the chart determines its acceptability immediately.

The evaluation charts for surface flaws are shown in figures A-2 and A-3, for circumferential and axial flaws, respectively. If the indication is determined to be embedded, the proper chart to use is figure A-4. The heavy diagonal line in figure A-4 can be used directly to determine whether the indication should be characterized as an embedded flaw or whether it is sufficiently close to the surface that it must be considered as a surface flaw (by the rules of Section XI). If the flaw parameters produce a plotted point below the heavy diagonal line, it is embedded and its acceptability is judged relative to the limit lines on the embedded flaw chart (figure A-4). If it is above the line, it must be considered a surface flaw, and evaluated using the charts for surface flaws, which appear in figures A-2 and A-3.

A detailed example on the use of the charts for a surface flaw is presented in the following section for a flaw in the elbow to valve weld region. It is followed by an embedded flaw example.

Surface Flaw Example

Now suppose the indication discussed in the body of this report is to be evaluated using the charts. For the circumferential orientation:

$$\begin{aligned} a &= 0.51" & \ell &= 1.5" \\ t &= 2.55" \end{aligned}$$

The flaw characterization parameters then become:

$$\begin{aligned} a/t &= 0.20 \\ a/\ell &= 0.34 \end{aligned}$$

Plotting these parameters on the surface flaw evaluation chart of figure A-2, it is quickly seen that the indication is acceptable.

Embedded Flaw Example

This discussion provides a sample calculation which explains the methods used to justify an example embedded flaw. An indication postulated to occur in the elbow to valve weld region has the following geometry:

$$\begin{aligned} a &= 0.16 \text{ in.} \\ \ell &= 1.6 \text{ in.} \end{aligned}$$

$$\text{Aspect Ratio} = a/\ell = 0.10$$

$$\begin{aligned} S &= 0.164 \text{ in.} \\ \delta &= S + a = 0.324 \text{ in.} \end{aligned}$$

t = thickness = 2.55 in.
 a/t = 0.063
 δ/t = 0.127

Plotting these parameters directly on the embedded flaw evaluation chart for this region, in figure A-4, it may be seen directly that the indication is acceptable.

Now that use of the charts has been illustrated, the following two sections will describe how they are constructed.

A-3 SURFACE FLAW EVALUATION

The acceptance criteria for surface flaws have been presented in Section 1 of the main report. For flaw evaluation in stainless steels, only the fatigue crack growth results must be calculated. The allowable flaw depths are determined directly from the tables in IWB 3640.

A-3.1 Fatigue Crack Growth

The first set of data required for surface flaw chart construction is the final flaw size a_f . As defined in IWB-3611 of ASME Code Section XI, a_f is the maximum flaw depth resulting from growth during a specific time period, which can be the next scheduled inspection of the component, or until the end of design lifetime. Therefore, the final depth, a_f after a specific service period of time must be used as the basis for evaluation. The charts are constructed to allow the initial (measured) indication size to be used directly. Charts have been constructed for operational periods of 10, 20, and 30 years from the time of detection.

The final flaw size a_f can be calculated by fatigue crack growth analysis, which has been performed covering the range of postulated flaw sizes, and flaw shapes at various locations of the components needed for the construction of surface flaw evaluation charts. The crack growth calculational methods have been discussed in section 4 of the report.

Notice that all the finite surface flaws and embedded flaws analyzed are semi-elliptical in shape. Crack growth analyses for finite surface flaws with aspect ratio (length to depth) less than 6:1 have utilized the results of 6:1, and for any flaw with aspect ratio larger than 6:1, the results of the continuous flaw are used. This is conservative in both cases.

A-3.2 Allowable Flaw Size Determination

The allowable flaw size for stainless steel is obtained directly from tables in paragraph IWB 3640, so the evaluation process is very straight forward. The allowable flaw size is calculated based on the most limiting transient for all normal operating conditions. Similarly, the allowable flaw size for emergency and faulted conditions is determined. The theory and methodology for the calculation of the allowable flaw sizes have been provided in section 3 and reference 4. Allowable flaw sizes were calculated for a range of flaw shapes, ranging from a continuous surface flaw ($a/l = 0$) to a semi-circle ($a/l = 0.5$).

A-3.3 Typical Surface Flaw Evaluation Chart

The two basic dimensionless parameters, which can fully address the characteristics of a surface flaw, were used for the evaluation chart construction. Namely,

- o Flaw Shape Parameter a/l or aspect ratio (AR) = l/a
- o Flaw Depth Parameter a/t

where,

- t = wall thickness, in.
- a = flaw depth, in.
- l = flaw length, in.

A typical chart was chosen for illustration purposes as follows: (Refer to Figure A-2)

- o The flaw shape parameter a/ℓ was plotted as the abscissa from 0 (continuous flaw) to .5 (AR = 2.). For values of a/ℓ which exceed 0.5, use the results for $a/\ell = 0.5$.
- o The flaw depth parameter a/t was plotted as the ordinate.
- o The lower curve is the code acceptable flaw depth tabulated in Table IWB-3514-2 of Section XI. These curves indicate the acceptance standards of the code, below which analytical evaluation is not required.
- o The upper boundary curve shows the maximum acceptable flaw depth based on flaw evaluation, beyond which no surface flaw is acceptable for continued service without repair. This upper bound curve has been determined by the fracture and fatigue evaluations described herein.
- o Any surface indication which falls between the two boundary curves will be acceptable by the code rules, based on the analytical justification provided herein. However, IWB-2420 of ASME Section XI requires future monitoring of such indications.

A-4 EMBEDDED FLAW EVALUATION

Embedded flaw evaluations were also performed in the form of flaw evaluation charts for indications in the elbow to valve weld region. This section describes the development of the embedded flaw charts for that region, which will also be useful for future inspections.

A-4.1 Methods of Evaluation

As with surface flaws, the allowable embedded flaw for the applicable loadings may be determined from tables in IWB-3640.

The stress intensity factors used for the crack growth calculations for embedded flaws were taken from reference A-1. These expressions developed by Shah and Kobayashi have been shown by the work of Lee and Bamford [A-2] to be very accurate for a range of flaw shapes, sizes and locations.

A-4.2 Embedded vs. Surface Flaws

According to IWA-3300 of the ASME Code Section XI a flaw is defined as embedded whenever:

$$S \geq 0.4a$$

where

S = the minimum distance from the flaw edge to the nearest vessel wall surface

a = the embedded flaw depth, (defined as the semi-minor axis of the elliptical flaw.)

The maximum embedded flaw size (a_0) for any given distance between the flaw centerline and the vessel wall surface (δ) as shown in Figure A-1, is found by the following process:

$$a = \delta - S \text{ (by definition)}$$

The limiting case for a flaw to be considered embedded is $S = 0.4a$, so substituting into the first equation, we find

$$\delta \geq 1.4a$$

Therefore, the limit for a flaw to be considered embedded is $a_0 = 0.714 \delta$. The demarcation line between the two domains is shown graphically in Figure A-4. Any flaw lying above the demarcation line should be evaluated as a surface flaw.

A-5 FLAW CHARTS - ELBOW TO VALVE WELD REGION

A-5.1 SURFACE FLAWS

The geometry and terminology for surface flaws at this weld is depicted in figure A-1. The following parameters must be determined for surface flaw evaluation with the charts

- o Flaw shape parameter $\frac{a}{l}$
- o Flaw depth parameter $\frac{a}{t}$

where a = The surface flaw depth detected (in.)
 l = The surface flaw length detected (in.)
 t = Wall thickness at the hot leg elbow to valve weld (t = 2.55")

The surface flaw evaluation charts for the hot leg elbow to valve weld are listed below:

- o Figure A-2 Evaluation Chart for Hot Leg Elbow to Valve Weld

<u>X</u>	Inside Surface	<u>X</u>	Surface Flaw	___	Longitudinal Flaw
___	Outside Surface	___	Embedded Flaw	<u>X</u>	Circumferential Flaw

- o Figure A-3 Evaluation Chart for Hot Leg Elbow to Valve Weld

<u>X</u>	Inside Surface	<u>X</u>	Surface Flaw	<u>X</u>	Longitudinal Flaw
___	Outside Surface	___	Embedded Flaw	___	Circumferential Flaw

A-5.2 EMBEDDED FLAWS

The geometrical description of an embedded flaw at the hot leg elbow to valve weld is depicted in figure A-1.

Basic Data:

- t = 2.55 in.
- δ = Distance of the centerline of the embedded flaw to the surface (in.)
- a = Flaw depth (defined as one half of the minor diameter) (in.)
- l = Flaw length (major diameter) (in.)
- a_o = Maximum embedded flaw size in depth direction, beyond which it must be considered a surface flaw, per Section XI characterization rules.

The following parameters must be calculated from the above dimensions to use the charts for evaluating the acceptability of an embedded flaw

- o Flaw shape parameter, $\frac{a}{l}$
- o Flaw depth parameter, $\frac{a}{t}$
- o surface proximity parameter, $\frac{\delta}{t}$

The evaluation chart for embedded flaws:

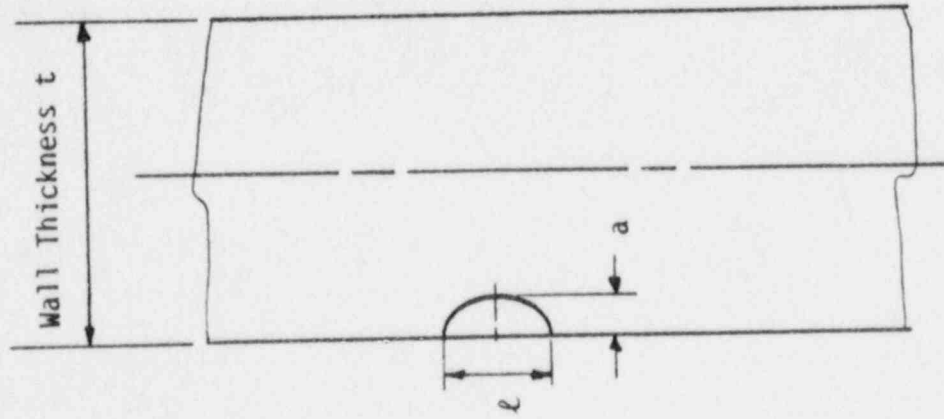
- o Figure A-4 Evaluation Chart for Hot Leg Elbow to Valve Weld
 - X Inside Surface ___ Surface Flaw ___ Longitudinal Flaw
 - X Outside Surface X Embedded Flaw X Circumferential Flaw

- o Figure A-5 Evaluation Chart for Hot Leg Elbow to Valve Weld
 - X Inside Surface ___ Surface Flaw Y Longitudinal Flaw
 - X Outside Surface X Embedded Flaw ___ Circumferential Flaw

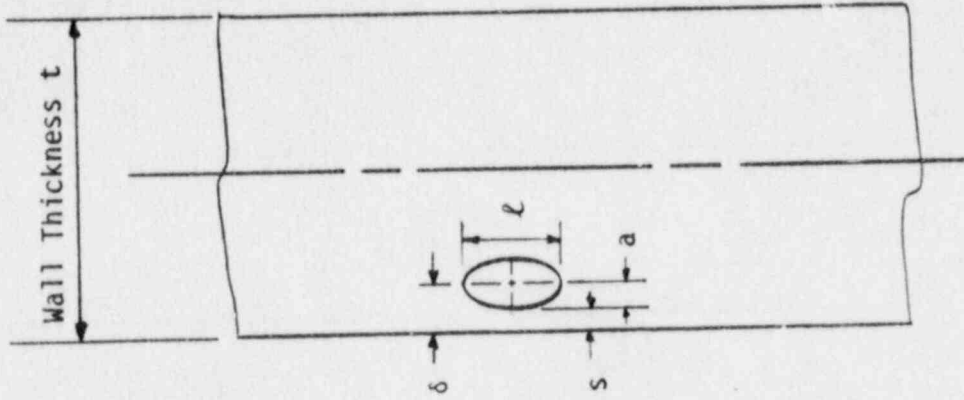
A-6 REFERENCES

- A.1 Shah, R. C. and Kobayashi, A. S., "Stress Intensity Factor for an Elliptical Crack Under Arbitrary Loading", Engineering Fracture Mechanics, Vol. 3, 1981, pp. 71-96.
- A.2 Lee, Y. S. and Bamford, W. H., "Stress Intensity Factor Solutions for a Longitudinal Buried Elliptical Flaw in a Cylinder Under Arbitrary Loads", presented at ASME Pressure Vessel and Piping Conference, Portland Oregon, June 1983. Paper 83-PVP-92.

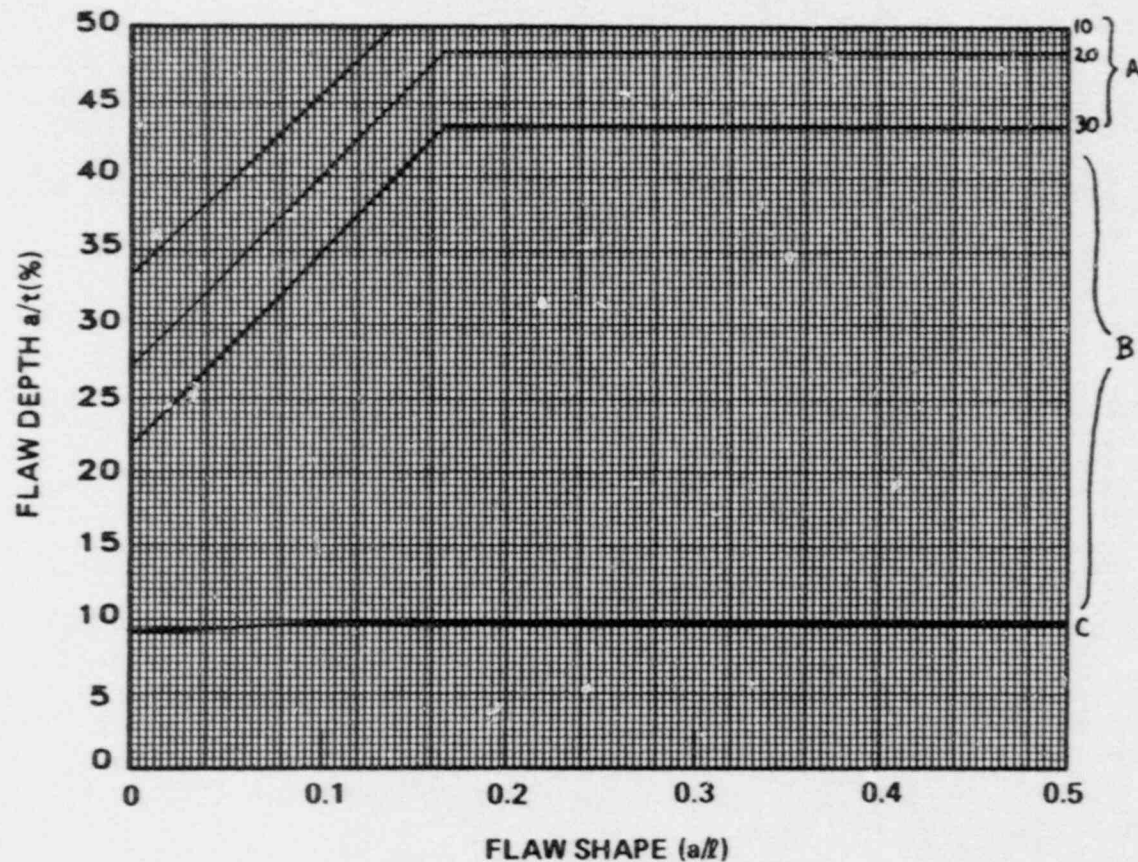
Figure A-1. Typical Notation for Surface and Embedded Flaw Indications



TYPICAL SURFACE FLAW INDICATION



TYPICAL EMBEDDED FLAW INDICATION

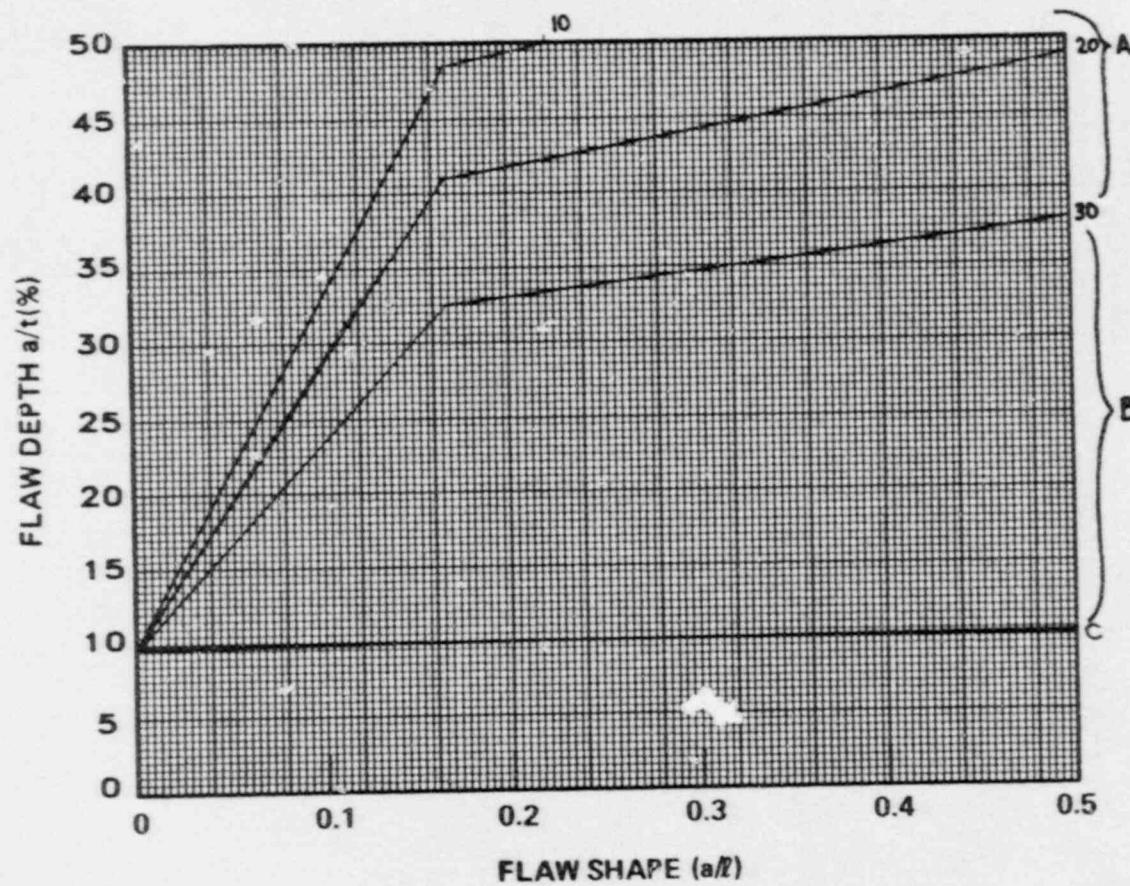


LEGEND

- A - The 10, 20, 30 year acceptable flaw limits.
- B - Within this zone, the surface flaw is acceptable by ASME Code analytical criteria in IWB-3600.
- C - ASME Code allowable - per Table IWB 3514-2.

Figure A-2 Evaluation Chart for Elbow to Valve Weld

<u>X</u>	Inside Surface	<u>X</u>	Surface Flaw	—	Longitudinal Flaw
—	Outside Surface	—	Embedded Flaw	<u>X</u>	Circumferential Flaw



LEGEND

- A - The 10, 20, 30 year acceptable flaw limits.
- B - Within this zone, the surface flaw is acceptable by ASME Code analytical criteria in IWB-3600.
- C - ASME Code allowable - per Table IWB 3514-2.

Figure A-3 Evaluation Chart for Elbow to Valve Weld

<u>X</u>	Inside Surface	<u>X</u>	Surface Flaw	<u>X</u>	Longitudinal Flaw
—	Outside Surface	—	Embedded Flaw	—	Circumferential Flaw

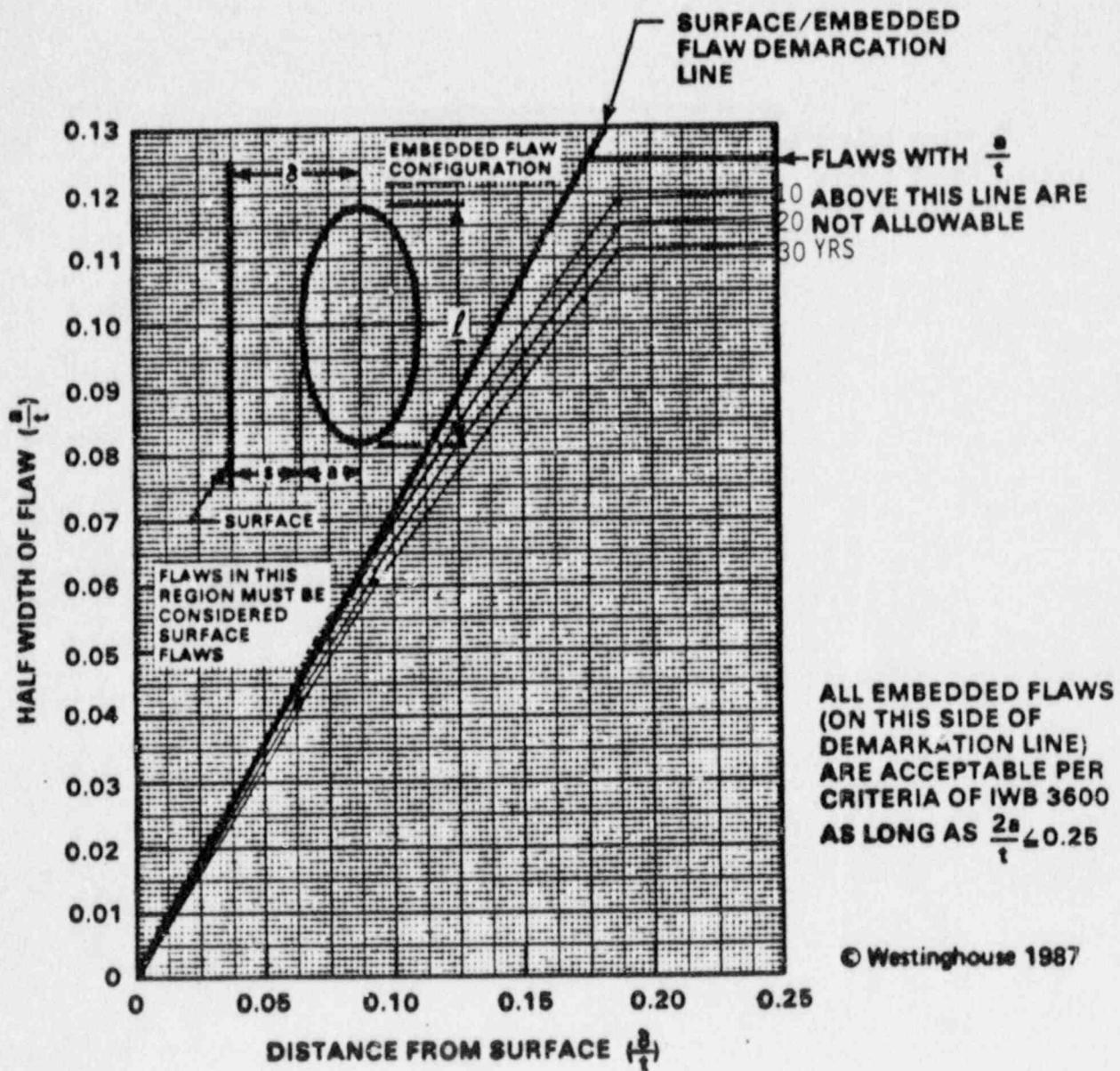


Figure A-4 Evaluation Chart for Elbow to Valve Weld

<u>X</u>	Inside Surface	—	Surface Flaw	—	Longitudinal Flaw
<u>X</u>	Outside Surface	<u>X</u>	Embedded Flaw	<u>X</u>	Circumferential Flaw

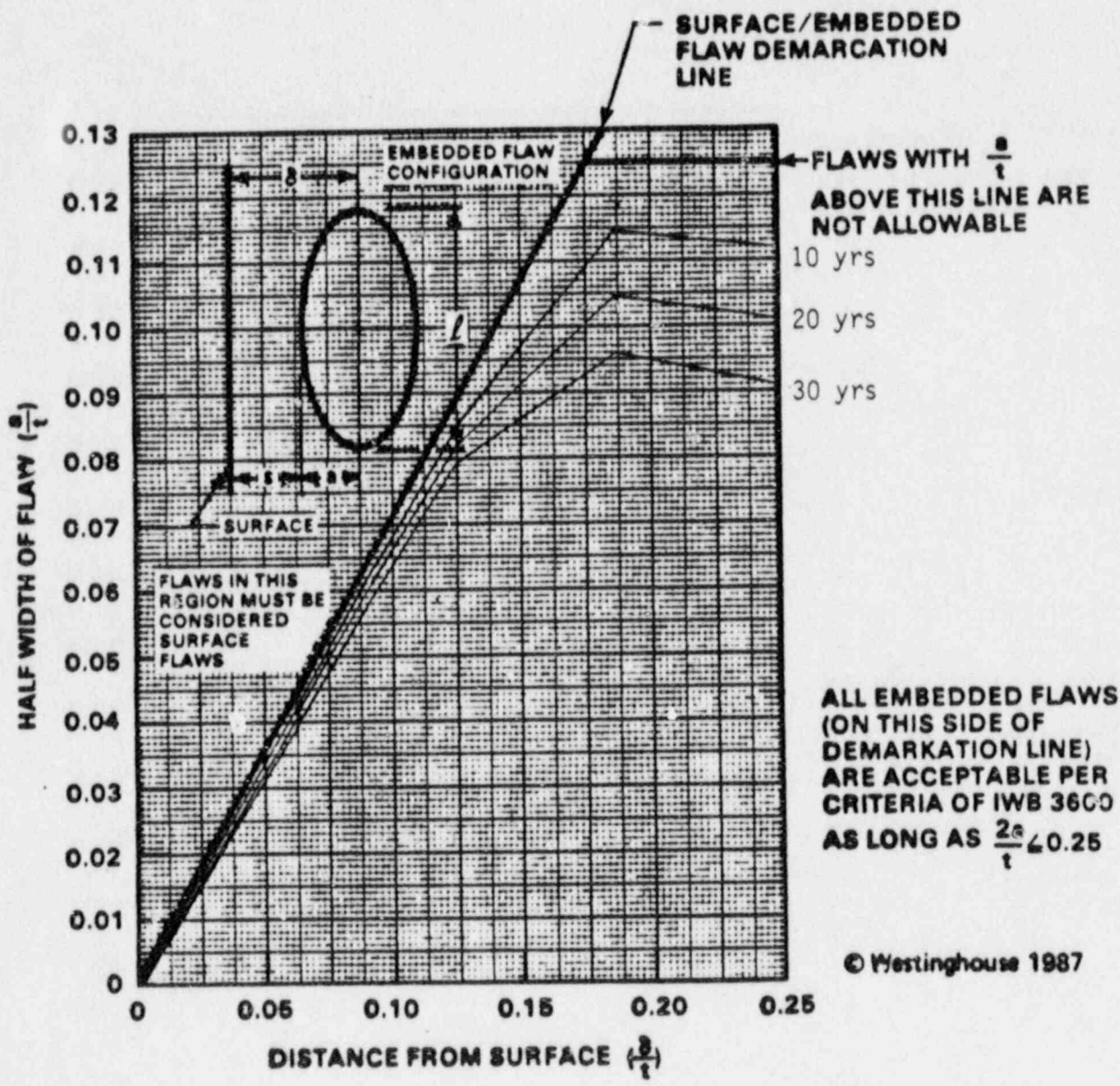


Figure A-5 Evaluation Chart for Elbow to Valve Weld

- | | | | | | |
|----------|-----------------|-------------|---------------|-------------|----------------------|
| <u>X</u> | Inside Surface | <u> </u> | Surface Flaw | <u>X</u> | Longitudinal Flaw |
| <u>X</u> | Outside Surface | <u>X</u> | Embedded Flaw | <u> </u> | Circumferential Flaw |